J|A|C|S
ARTICLES
Published on Web 06/01/2002

Improper or Classical Hydrogen Bonding? A Comparative Cryosolutions Infrared Study of the Complexes of $HCClF_2$, $HCCl_2F$, and $HCCl_3$ with Dimethyl Ether

Sofie N. Delanoye, Wouter A. Herrebout, and Benjamin J. van der Veken*

Contribution from the Department of Chemistry, Universitair Centrum Antwerpen, Groenenborgerlaan 171, B-2020 Antwerp, Belgium

Received November 12, 2001

Abstract: Complexes of haloforms of the type $HCCl_nF_{3-n}$ ($n = 1-3$) with dimethyl ether have been studied in liquid argon and liquid krypton, using infrared spectroscopy. For the haloform C−H stretching mode, the complexation causes blue shifts of 10.6 and 4.8 cm^{-1} for $HCClF_2$ and $HCCl_2F$, respectively, while for $HCCl_3$ a red shift of 8.3 cm^{-1} is observed. The ratio of the band areas of the haloform C−H stretching in complex and monomer was determined to be 0.86(4) for $HCClF_2$, 33(3) for $HCCl_2F$, and 56(3) for $HCCl_3$. These observations, combined with those for the HCF_3 complex with the same ether (*J. Am. Chem. Soc.* **2001**, *123*, 12290), have been analyzed using ab initio calculations at the MP2=FC/6-31G(d) level, and using some recent models for improper hydrogen bonding. Ab initio calculations on the haloforms embedded in a homogeneous electric field to model the influence of the ether suggest that the complexation shift of the haloform C−H stretching is largely explained by the electric field effect induced by the electron donor in the proton donor. The model calculations also show that the electric field effect accounts for the observed intensity changes of the haloform C−H stretches.

Introduction

The weak interaction of C−H bonds with lone-pair electrons of oxygen and nitrogen atoms in various molecules makes itself felt in areas as diverse as the structure of biomolecules[1−3] and crystal engineering.[4,5] As a consequence, the properties of weakly bound complexes involving these interactions have been the subject of intense research; a variety of complexes involving C−H...O and C−H...N interactions have been studied theoretically, using semiempirical[6] or ab initio calculations,[7−20] and experimentally, using crystallography,[21] rotational,[22−24] vibrational,[25−32] or NMR spectroscopy.[33] These studies have shown that, in some cases, the C−H bond in the proton donor molecule is weakened during the complexation, but that, in other cases, this bond is somewhat strengthened.

The weakening of the C−H bond in the first type of complexes is accompanied by a red shift of the C−H stretching fundamental and a significant increase of its infrared intensity. These are the properties traditionally associated with X−H...Y hydrogen bonds. This type of interaction is described as *classical hydrogen bonding.*[15]

Because of the strengthening of the C−H bond, the second type of complexes is characterized by a blue shift of the C−H

* To whom correspondence should be addressed. E-mail: bvdveken@ruca.ua.ac.be. Fax: int-32-3-2180233.

(1) Weiss, M. S.; Brandl, M.; Suhnel, J.; et al. *Trends Biochem. Sci.* **2001**, *26*, 521.
(2) Brandl, M.; Meyer, M.; Suhnel, J. *J. Biomol. Struct. Dyn.* **2001**, *18*, 545.
(3) Scheiner, S.; Kar, T.; Gu, Y. *J. Biol. Chem.* **2001**, *276*, 9832.
(4) Desiraju, G. R.; Steiner, T. *The Weak Hydrogen Bond in Structural Chemistry and Biology*; Oxford university Press: New York, 1999.
(5) Harder, S. *Chem.-Eur. J.* **1999**, *5*, 1852.
(6) Dannenberg, J. J. *J. Mol. Struct. (THEOCHEM)* **1997**, *401*, 279.
(7) Vargas, R.; Garza, J.; Friesner, R. A.; Stern, H.; Hay, B. P.; Dixon, D. A. *J. Phys. Chem. A* **2001**, *105*, 4963.
(8) Scheiner, S.; Gu, Y.; Kar, T. *J. Mol. Struct. (THEOCHEM)* **2000**, *500*, 441.
(9) Salvador, P.; Simon, S.; Duran, M.; Dannenberg, J. J. *J. Chem. Phys.* **2000**, *113*, 5666.
(10) Scheiner, S. *Adv. Mol. Struct. Res.* **2000**, *6*, 159.
(11) Muller-Dethlefs, K.; Hobza, P. *Chem. Rev.* **2000**, *100*, 143.
(12) Masunov, A.; Dannenberg, J. J.; Contreras, R. H. *J. Phys. Chem. A* **2001**, *105*, 4737.
(13) Kryachko, E. S.; Zeegers-Huyskens, T. *J. Phys. Chem. A* **2001**, *105*, 7118.
(14) Hobza, P. *Phys. Chem. Chem. Phys.* **2001**, *3*, 2555.
(15) Hobza, P.; Havlas, Z. *Chem. Rev.* **2000**, *100*, 4253.
(16) Hartmann, M.; Wetmore, S. D.; Radom, L. *J. Phys. Chem. A* **2001**, *105*, 4470.
(17) Gu, Y.; Kar, T.; Scheiner, S. *J. Am. Chem. Soc.* **1999**, *121*, 9411.
(18) Dannenberg, J. J.; Haskamp, L.; Masunov, A. *J. Phys. Chem. A* **1999**, *103*, 7083.
(19) Cubero, E.; Oroczo, M.; Hobza, P.; Luque, F. J. *J. Phys. Chem. A* **1999**, *103*, 6394.
(20) Cubero, E.; Orozco, M.; Luque, F. J. *Chem. Phys. Lett.* **1999**, *310*, 445.
(21) Jeffrey, G. A. *J. Mol. Struct.* **1999**, *485−486*, 293.
(22) Fraser, G. T.; Lovas, F. J.; Suenram, R. D.; Nelson, D. D.; Klemperer, W. *J. Chem. Phys.* **1986**, *84*, 5983.
(23) Caminati, W.; Melandri, S.; Moreschini, P.; Favero, P. G. *Angew. Chem., Int. Ed.* **1999**, *38*, 2924.
(24) Legon, A. C. *Chem. Phys. Lett.* **1995**, *247*, 24.
(25) Tokhadze, K. G.; Tkhorzhevskaya, N. A. *J. Mol. Struct.* **1986**, *32*, 11.
(26) Marques, M. P. M.; Amorin da Costa, A. M.; Ribeiro-Claro, P. J. A. *J. Phys. Chem. A* **2001**, *105*, 5292.
(27) Jemmis, E. D.; Giju, K. T.; Sundararajan, K.; Sankaran, K.; Vidya, V.; Viswanathan, K. S.; Leszczynski, J. *J. Mol. Struct.* **1999**, *510*, 59.
(28) Chang, H.-C.; Jiang, J.-C.; Lin, S. H.; Weng, N.-H.; Chao, M.-C. *J. Chem. Phys.* **2001**, *115*, 3215.
(29) Boldeskul, I. E.; Tsymbal, I. F.; Ryltsev, E. V.; Latajka, Z.; Barnes, A. J. *J. Mol. Struct.* **1997**, *436−437*, 167.
(30) Bedell, B. L.; Goldfarb, L.; Mysak, E. R.; Samet, C.; Maynard, A. *J. Phys. Chem. A* **1999**, *103*, 4572.
(31) Antonenko, G. V.; Kolomiytsova, T. D.; Kondaurov, V. A.; Shchepkin, D. N. *J. Mol. Struct.* **1992**, *275*, 183.
(32) Mizuno, K.; Ochi, T.; Shindo, Y. *J. Chem. Phys.* **1998**, *109*, 9502.
(33) Giribet, C. G.; Vizioli, C.; Ruiz de Azua, M. C.; Contreras, R. H.; Dannenberg, J. J.; Masunov, A. *J. Chem. Soc., Faraday Trans.* **1996**, *92*, 3029.

10.1021/ja0125220 CCC: $22.00

stretching fundamental. Moreover, for complexes involving HCF_3, this shift is often accompanied by a significant decrease of its infrared intensity.[3,8,10,15] The properties of these complexes thus are opposite to those for classical hydrogen bonding and are, therefore, described as *anti-hydrogen bonding* or *blue-shifting, improper hydrogen bonding*.[15]

The nature of the blue-shifting, improper hydrogen bonds has recently caught the attention of several theoretical groups, and is the subject of intense discussion. On the basis of results derived from natural bond orbital (NBO) analyses, Hobza and co-workers[15,34−36] recently suggested that the blue-shifting hydrogen bonds are completely different from the classical ones. According to these authors, the improper hydrogen bonds must be regarded as a new type of bonding. This viewpoint, however, is not shared by others.[3,8,10,13,17,37] S. Scheiner et al.[3,8,10,17,37] have compared a variety of chemical properties, including complexation energies, vibrational spectra, charge distributions, and NMR chemical shifts for typical C−H...O and C−H...N interactions and for standard O−H...O hydrogen-bonded species, and have concluded that there is no fundamental distinction between the different interactions. From a different point of view, light has been shed on classical and improper hydrogen bonding by Dannenberg et al.,[12] who investigated, using ab initio methods, the effect of electric fields on proton donors.

The ultimate test for a unified model of hydrogen bonding is to see how well the underlying theories are capable of rationalizing experimental data on unusual hydrogen bonding. Although by now several nonclassical hydrogen bonds have been described in the literature, their number is several orders of magnitude smaller than the number of well-documented cases of classical hydrogen bonding. The present study is an attempt to contribute a few more cases to the former class.

We have recently shown[36] that the bonding in the complex of fluoroform, HCF_3, with dimethyl ether, $(CH_3)_2O$, is of the improper type; the haloform C−H stretching mode blue shifts by 17.7 cm^{-1} when the complex is formed, while its monomer-to-complex intensity ratio was found to be 11(2).[36] Chloroform, $HCCl_3$, on the other hand, with a few recently described exceptions,[29,34] forms complexes involving classical hydrogen bonding; more than 75 of them have been collected in R. D. Green's early review[38] of hydrogen bonding by C−H groups. If the complex of chloroform with dimethyl ether would be of the classical type, it is not unrealistic to expect that the complexes of the mixed haloforms $HCClF_2$ and $HCCl_2F$ with the same electron donor show a systematic transition from improper to classical hydrogen bonding. Experimental evidence for such a transition has hitherto not been described, and it is not unreasonable to expect that it would throw new light on hydrogen bonding in general. Therefore, in this study we have investigated the infrared spectra of solutions in liquid argon and krypton of dimethyl ether and the above haloforms. In the next paragraphs, we will show that for each haloform a complex has been observed. The frequency and intensity behavior of the haloform C−H stretching have been measured, and it will be shown that a systematic trend indeed is detected. The observed spectral properties will be compared with ab initio calculations on the complexes, and their evolution in the series will be interpreted in light of recent models of hydrogen bonding.

Experimental Section

Vibrational Spectroscopy. The haloforms and dimethyl ether were obtained from Sigma Aldrich, and have a stated purity of 99.9+% ($HCClF_2$), 98% ($HCCl_2F$), 99.9% ($HCCl_3$), 99+% (dimethyl ether), and 99.8 atom % ($DCCl_3$). All compounds were used without further purification.

The cryosolution setup consists of a 1 cm copper cell, suspended in a vacuum shroud, and equipped with wedged silicon windows. The cell is cooled with boiling liquid nitrogen and is connected to a pressure manifold for filling and evacuation. Solutions were prepared by first condensing the monomers in the cooled cell, followed by condensation of the solvent gas. The latter process causes strong turbulence, so that no extra mixing was required. The solvent gases, argon and krypton, were provided by L'Air Liquide and have a stated purity of 99.9999% and 99.998%, respectively.

Infrared spectra were recorded on a Bruker IFS 66v spectrometer, using a globar source, a Ge/KBr beam splitter, and a broad band MCT detector. For each spectrum, 200 interferograms were averaged, Blackman-Harris 3-Term apodized, and Fourier transformed with a zero filling factor of 8 to produce a spectrum with a resolution of 0.5 cm^{-1}.

Ab Initio Calculations. In a recent review[15] on improper hydrogen bonding, P. Hobza and Z. Havlas stressed the fact that accurate information on the geometry and the vibrational frequencies of weakly bound species involving C−H...O interactions should only be obtained from BSSE-corrected potential energy surfaces. Therefore, in this study the equilibrium geometry of the different complexes studied and the corresponding vibrational frequencies were calculated using a modified version of the CP-optimizer package developed by P. Salvador,[39] because it allows a user-friendly interface to the Gaussian 98[40] program. The different algorithms required during these calculations have been described in the literature.[41−46] The calculations were performed at the MP2=FC/6-31G(d) level.

Results

Monomer Spectra. The vibrational spectra of the monomers dissolved in liquefied rare gases or trapped in solid matrixes have been described before, and will not be discussed in detail here.[47−53] One peculiarity, however, should be mentioned. In a

(34) Hobza, P.; Spirko, V.; Havlas, Z.; Buchhold, K.; Reimann, B.; Barth, H.-D.; Brutschy, B. *Chem. Phys. Lett.* **1999**, *299*, 180.
(35) Reimann, B.; Buchhold, K.; Vaupel, S.; Brutschy, B.; Havlas, Z.; Spirko, V.; Hobza, P. *J. Phys. Chem. A* **2001**, *105*, 5560.
(36) Van der Veken, B. J.; Herrebout, W. A.; Szostak, R.; Shchepkin, D. N.; Havlas, Z.; Hobza, P. *J. Am. Chem. Soc.* **2001**, *123*, 12290.
(37) Scheiner, S.; Kar, T. *J. Phys. Chem. A* **2002**, *106*, 1784.
(38) Green, R. D. *Hydrogen Bonding by C−H Groups*; Macmillan: London, 1974.
(39) Salvador, P. http://iqc.udg.es/~perico/bbopt.html.
(40) Frisch, M. J.; Trucks, G. W.; Schlegel, H. B.; Scuseria, G. E.; Robb, M. A.; Cheeseman, J. R.; Zakrzewski, V. G.; Montgomery, J. A., Jr.; Stratmann, R. E.; Burant, J. C.; Dapprich, S.; Millam, J. M.; Daniels, A. D.; Kudin, K. N.; Strain, M. C.; Farkas, O.; Tomasi, J.; Barone, V.; Cossi, M.; Cammi, R.; Mennucci, B.; Pomelli, C.; Adamo, C.; Clifford, S.; Ochterski, J.; Petersson, G. A.; Ayala, P. Y.; Cui, Q.; Morokuma, K.; Malick, D. K.; Rabuck, A. D.; Raghavachari, K.; Foresman, J. B.; Cioslowski, J.; Ortiz, J. V.; Stefanov, B. B.; Liu, G.; Liashenko, A.; Piskorz, P.; Komaromi, I.; Gomperts, R.; Martin, R. L.; Fox, D. J.; Keith, T.; Al-Laham, M. A.; Peng, C. Y.; Nanayakkara, A.; Gonzalez, C.; Challacombe, M.; Gill, P. M. W.; Johnson, B. G.; Chen, W.; Wong, M. W.; Andres, J. L.; Head-Gordon, M.; Replogle, E. S.; Pople, J. A. *Gaussian 98*, revision A.5; Gaussian, Inc.: Pittsburgh, PA, 1998.
(41) Simon, S.; Duran, M.; Dannenberg, J. J. *J. Chem. Phys.* **1996**, *105*, 11024.
(42) Simon, S.; Bertran, J.; Sodupe, M. *J. Phys. Chem. A* **2001**, *105*, 4359.
(43) Salvador, P.; Simon, S.; Duran, M.; Dannenberg, J. J. *J. Chem. Phys.* **2000**, *113*, 5666.
(44) Salvador, P.; Paizs, B.; Duran, M.; Suhai, S. *J. Comput. Chem.* **2001**, *22*, 765.
(45) Salvador, P.; Fradera, X.; Duran, M. *J. Chem. Phys.* **2000**, *112*, 10106.
(46) Salvador, P.; Duran, M. *J. Chem. Phys.* **1999**, *111*, 4460.
(47) Zhigula, L. A.; Kolomiitsova, T. D.; Melikova, S. M.; Shchepkin, D. N. *J. Appl. Spectrosc.* **1997**, *64*, 310.
(48) Mielke, Z.; Wierzejewska, M.; Olbert, A.; Krajewska, M.; Tokhadze, K. G. *J. Mol. Struct.* **1997**, *436−437*, 339.
(49) McLaughlin, J. G.; Poliakoff, M.; Turner, J. J. *J. Mol. Struct.* **1982**, *82*, 51.

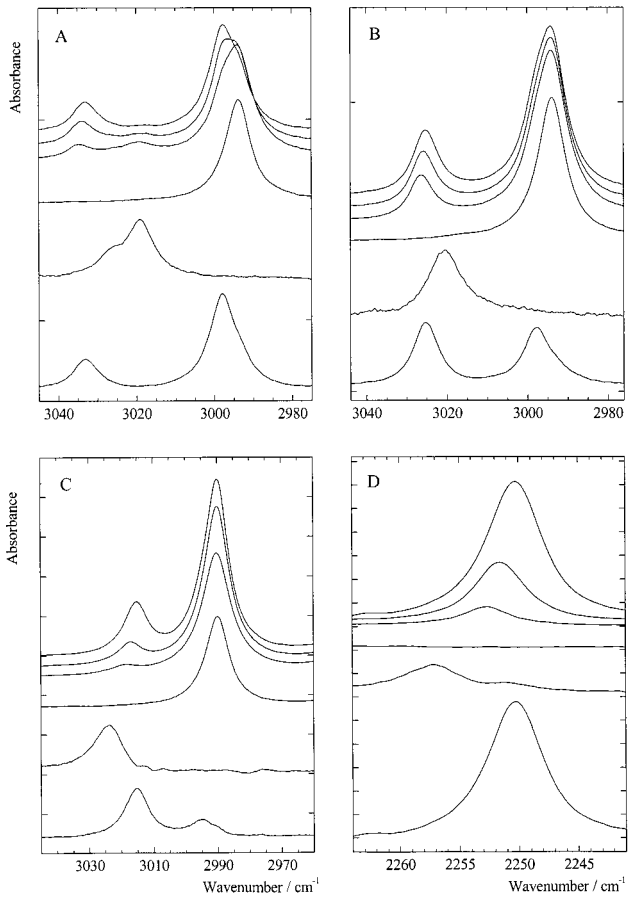

Figure 1. Infrared spectra of cryosolutions in the region of the C−H/D stretches. (A) The top three spectra are of a solution in liquid argon containing both dimethyl ether and $HCClF_2$, both with mole fractions equal to 1.7×10^{-4}; from top to bottom the temperatures are 100, 112, and 123 K; the next two traces are the spectra of a solution containing only dimethyl ether, and that of a solution containing only $HCClF_2$, respectively, both at 100 K; the bottom trace is the spectrum of the 1:1 complex, at 100 K, isolated by subtraction techniques. (B) The top three spectra are of a solution in liquid argon containing both dimethyl ether, with a mole fraction equal to 1.0×10^{-4}, and $HCCl_2F$, with a mole fraction equal to 0.5×10^{-4}; from top to bottom the temperatures are 100, 112, and 123 K; the next two traces are the spectra of a solution containing only dimethyl ether, and that of a solution containing only $HCCl_2F$, respectively, both at 100 K; the bottom trace is the spectrum of the 1:1 complex, at 100 K, isolated by subtraction techniques. (C) The top three spectra are of a solution in liquid krypton containing both dimethyl ether, with a mole fraction equal to 2.9×10^{-4}, and $HCCl_3$, with a mole fraction equal to 1.0×10^{-4}; from top to bottom the temperatures are 125, 145, and 165 K; the next two traces are the spectra of a solution containing only dimethyl ether, and that of a solution containing only $HCCl_3$, respectively, both at 125 K; the bottom trace is the spectrum of the 1:1 complex, at 145 K, isolated by subtraction techniques. (D) The same as in (C), but using $DCCl_3$, with a mole fraction of 2.9×10^{-4} for the haloform.

recent paper, Zhigula et al.[47] have reported on the vibrational spectra of a variety of Freons dissolved in liquid argon. For $HCClF_2$, a single band in the fundamental C−H stretching region was reported to appear, at 3018.2 cm^{-1}.[47] In the spectra recorded in this study, two separate bands can be observed, a more intense band at 3019.2 cm^{-1} and a weaker shoulder at 3026.1 cm^{-1}, as is clear from Figure 1A. The presence of a second transition is in agreement with the vapor phase spectra of this compound,[54−57] in which Q branches have been assigned at 3021.6 and 3024.6 cm^{-1}. Despite several attempts, no definitive assignment of the level in resonance with the first excited state of the C−H stretching could be proposed.[55−57]

Complex Spectra. Infrared spectra of a series of mixtures in liquid argon and in liquid krypton containing mole fractions of DME ranging from 1.0×10^{-4} to 3.0×10^{-4} and containing the appropriate haloform with mole fractions between 0.5×10^{-4} and 3.0×10^{-4} were investigated. For each haloform, new bands were observed in the spectra of mixed solutions, which we assign to a 1:1 complex with DME. The frequencies observed for the haloform C−H and C−X stretches, and their complexation shifts, are collected in Table 1, while those observed for the other modes of the haloforms, and for DME, are summarized in Tables S1 and S2 of the Supporting Information.

In Figure 1, the CH stretching regions of monomer and mixed solutions are compared. The new bands in the spectra of the mixed solutions, although significantly overlapped by monomer bands, can be clearly observed. The new bands, that is, the spectra of the complexes, were isolated from those of the monomers by subtracting out monomer contributions, using monomer spectra recorded at identical temperatures. The difference spectra are given as the lowest trace in each panel.

The spectral region shown in Figure 1A−C has been chosen to include both the C−H stretching, that is, ν_1, of the haloform and the accidentally degenerate ν_1, ν_{12} doublet of DME at 2994 cm^{-1}. In the spectra of the complexes, the lower traces in Figure 1A−C, two bands are present. One appears consistently approximately 4 cm^{-1} above the ν_1, ν_{12} monomer DME doublet, which we assign to the corresponding modes in the complex. This leaves the second band to be associated with the haloform C−H stretching of the complex. For $HCClF_2$, this band appears at 3033.2 cm^{-1}, blue shifted from the monomer doublet. It appears as a singlet, suggesting that the anharmonic resonance that gives rise to the high-frequency shoulder in monomer ν_1 is strongly reduced. A possible explanation for this is that the mode interacting with ν_1 is shifted downward by the complexation, while ν_1 is shifted upward, these shifts destroying the resonance condition. Although the exact assignment of the mode interacting with ν_1 is uncertain,[55−57] it appears justified to treat the doublet as a Fermi resonance. By then assigning the more intense component as ν_1, the upper limit for the frequency of this mode in the monomer in absence of the resonance can be taken midway between the components of the doublet, at 3022.6 cm^{-1}. In this way, the blue shift of ν_1 upon complexation is found to be 10.6 cm^{-1}.

Comparison of the ν_1 monomer and complex frequencies shows that for $HCCl_2F$ the complexation induces a blue shift of 4.8 cm^{-1}, while for $HCCl_3$ a red shift, by 8.3 cm^{-1}, results. The results presented in Figure 1D for the complex between DME and $DCCl_3$ confirm the red shift for ν_1, which in this case is measured to be 6.9 cm^{-1}.

(50) Han, S. W.; Kim, K. *J. Mol. Struct.* **1999**, *475*, 43.
(51) Lefebvre, J. H.; Anderson, A. *J. Raman Spectrosc.* **1991**, *22*, 633.
(52) Goebel, J.; Ault, B. S.; Del Bene, J. E. *J. Phys. Chem. A* **2000**, *104*, 2033.
(53) Anderson, A.; Beardsall, A. J.; Fraser, J. M. *Phys. Status Solidi* **1994**, *182*, 59.
(54) Magill, J. V.; Gough, K. M.; Murphy, W. F. *Spectrochim. Acta, Part A* **1986**, *42*, 705.
(55) Fraser, G. T.; Domenech, J.; Junttila, M.-L.; Pine, A. S. *J. Mol. Spectrosc.* **1992**, *152*, 307.
(56) Brown, A.; McKean, D. C.; Duncan, J. L. *Spectrochim. Acta, Part A* **1988**, *44*, 553.
(57) Amrein, A.; Luckhaus, D.; Merkt, F.; Quack, M. *Chem. Phys. Lett.* **1988**, *152*, 275.

Table 1. Characteristic Frequencies (in cm^{-1}), Complexation Shifts (in cm^{-1}), and Intensity Ratios Obtained for the Different Complexes Formed between Dimethyl Ether and HCF_3, $HCClF_2$, $HCCl_2F$, and $HCCl_3$

	HCF_3			$HCClF_2$			$HCCl_2F$			$HCCl_3$		
	$\nu_{monomer}$	$\nu_{complex}$	$\Delta\nu$	$\nu_{monomer}$	$\nu_{complex}$	$\Delta\nu$	$\nu_{monomer}$	$\nu_{complex}$	$\Delta\nu$	$\nu_{monomer}$	$\nu_{complex}$	$\Delta\nu$
Observed Values												
C−H stretching	3036.7	3054.4	17.7	3019.2 3026.1	3033.2	14.0	3020.6	3025.4	4.8	3023.6	3015.3	−8.3
C−X stretching				804.3 800.3	795.5 792.0	−8.8 −8.3	1071.7	1064.5	−7.2			
CX_2 symm. stretching				1100.8	1091.9	−8.9	741.8 739.4	738.1 734.6 731.8	−3.7 −4.8			
CX_2 antisymm. stretching				1117.7	1108.6	−9.1	801.2 800.0	793.6 792.6	−7.6 −7.4			
CX_3 symm. stretching	1134.5	1122.4	−12.1							673.8 672.2 670.8	669.7 668.1 666.6	−4.1 −4.1 −4.2
CX_3 antisymm. stretching	1144.7	1132.6	−12.1							767.6	761.4	−6.2
Calculated Values												
C−H stretching	3234.8	3265.7	30.9	3228.4	3251.2	22.8	3231.1	3242.3	11.2	3243.0	3235.1	−7.9
C−X stretching				850.3	840.4	−9.9	1132.9	1124.9	−8.0			
CX_2 symm. stretching				1151.4	1142.2	−9.2	776.3	770.0	−6.3			
CX_2 antisymm. stretching				1190.1	1181.4	−8.7	855.5	846.4	−9.1			
CX_3 symm. stretching	1169.8	1160.6	−9.2							706.4	703.1	−3.3
CX_3 antisymm. stretching	1216.0 1216.0	1204.9 1205.9	−11.1 −10.1							823.7 823.2	817.6 816.7	−6.1 −6.5
					$\epsilon_{complex}/\epsilon_{monomer}$							
observed value in LAr		0.09(2)			0.86(4)			33(3)				
observed value in LKr					0.89(6)			26(1)			56(3)	
ab initio value		0.024			0.314			5.93			3976.7	

In view of the intensity changes of the infrared X−H stretching mode associated with hydrogen bonding, it is of interest to note the evolution of the relative intensities in Figure 1A−C; for DME·$HCClF_2$, the ν_1, ν_{12} DME doublet is approximately three times more intense than $\nu_1^{HCClF_2}$, while for DME·$HCCl_3$, this ratio is more than inversed. In a later paragraph, we will return to this aspect in a more quantitative way.

Recent reports have linked improper hydrogen bonding with significant charge transfer to atoms of the proton donor not directly involved in the hydrogen bond.[15,34−36] For fluoroform, charge transfer to the fluorine lone pairs has been calculated, and ab initio calculations reveal a concomitant decrease in the C−F stretching frequencies.[36] In view of this, we have paid some attention to the carbon−halogen stretches in the present complexes.

In Figure 2A, the C−F stretching region of a mixed DME/$HCClF_2$ solution is compared with those of the monomers. In the former, three complex bands are observed, at 1108.6, 1097.4, and 1091.9 cm^{-1}. For all complexes studied here, a band near 1097 cm^{-1} has been observed, which we associate with the 1100 cm^{-1} DME band. When we assign the remaining two complex bands in this region, in the same order as in the monomer, to the antisymmetric and symmetric CF_2 stretches, it is clear from Figure 2A that both modes red shift upon complexation, by approximately 9 cm^{-1}.

For $HCCl_2F$, the region of the symmetric C−Cl stretch, shown in Figure 2B, is complicated by isotopic splittings and by the presence of the $\nu_5 + \nu_6$ combination band.[47] Comparison of the spectra of monomers and complex, however, shows that all bands undergo a red shift upon complexation, by approximately 4.0 cm^{-1}. Similarly, in Figure 2C and D the isotopic multiplets due to the symmetric CCl_3 stretch in $HCCl_3$ and $DCCl_3$ can be seen to red shift upon complexation, by approximately 4 cm^{-1}. Data on the carbon−halogen stretches not shown in Figure 2 have, along with those discussed above, been collected in Table 1; it can be seen that also for these modes red shifts occur.

Figure 3 illustrates the behavior upon formation of the hydrogen bond of the ν_6 mode of DME in the different complexes. It can be seen that in all cases a red shift occurs, which increases slightly from the complex with $HCClF_2$, −6.6 cm^{-1}, to the complex with $HCCl_3$, −7.4 cm^{-1}, while in the complex with HCF_3 a shift of −6.4 cm^{-1} was observed[36] for this mode. It is not unrealistic to assume that the perturbation of DME by the haloform increases with increasing strength of the complexes and that the complexation shift of the ν_6 mode increases with increasing perturbation of DME. The results in Figure 3 then show that the strength of the complex increases from fluoroform to chloroform.

Intensities. The infrared intensity ratios $\epsilon_{complex}/\epsilon_{monomer}$ for the haloform CH stretchings were measured using band areas for these modes, measured at different temperatures. In a temperature run, the molar concentrations of monomer and complex change because of the temperature dependence of the complexation constant and because of the temperature variations of the density of the solution, but the total amount of haloform present remains constant. This can be expressed using infrared band areas as

$$I^{corr}_{complex} = -\frac{\epsilon_{complex}}{\epsilon_{monomer}} I^{corr}_{monomer} + c$$

in which $\epsilon_{complex}$ and $\epsilon_{monomer}$ are the infrared intensities, $I^{corr}_{complex}$ and $I^{corr}_{monomer}$ are density corrected band areas of the haloform C−H stretch in complex and monomer, respectively, and c is a constant. For the present study, the density corrections are necessary because in the temperature intervals used the densities of liquid argon and liquid krypton vary by about 15%

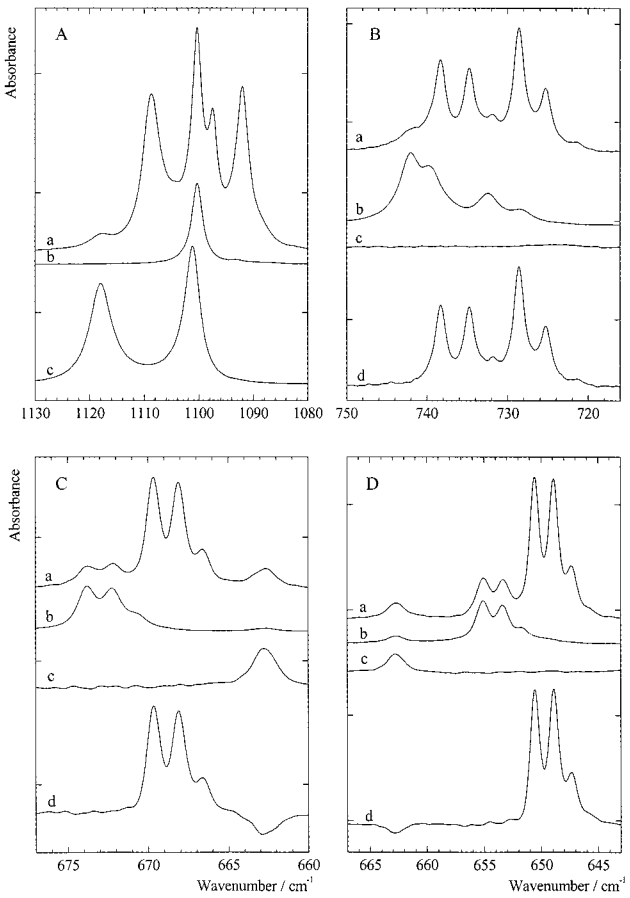

Figure 2. (A) Infrared spectra of solutions in liquid argon at 103 K, in the C−F stretching region: (a) solution containing dimethyl ether and $HCClF_2$, with mole fraction equal to 1.9×10^{-4} and 0.5×10^{-4}, respectively; (b) solution containing only dimethyl ether; (c) solution containing only $HCClF_2$. (B) Infrared spectra of solutions in liquid argon at 109 K, in the symmetric CCl_2 stretching region: (a) solution containing dimethyl ether and $HCCl_2F$, with mole fraction equal to 1.0×10^{-4} and 0.5×10^{-4}, respectively; (b) solution containing only $HCCl_2F$; (c) solution containing only dimethyl ether, (d) difference spectrum containing only complex bands. (C) Infrared spectra of solutions in liquid krypton at 124 K, in the symmetric CCl_3 stretching region: (a) solution containing dimethyl ether and $HCCl_3$, with mole fraction equal to 2.9×10^{-4} and 1.0×10^{-4}, respectively; (b) solution containing only $HCCl_3$; (c) solution containing only dimethyl ether, the band at 662.8 cm^{-1} is due to CO_2; (d) difference spectrum containing only complex bands. (D) Infrared spectra of solutions in liquid krypton at 125 K, in the symmetric CCl_3 stretching region: (a) solution containing dimethyl ether and $DCCl_3$, with mole fraction equal to 2.9×10^{-4}; (b) solution containing only $DCCl_3$; (c) solution containing only dimethyl ether, the band at 662.8 cm^{-1} is due to CO_2; (d) difference spectrum containing only complex bands.

and 10%, respectively.[58] At any temperature T, the density corrected band area $I_i^{corr}(T)$ was calculated from the experimental band area $I_i(T)$ as

$$I_i^{corr}(T) = I_i(T)\frac{\rho(T_R)}{\rho(T)}$$

in which $\rho(T)$ and $\rho(T_R)$ are the densities of the solution at temperature T and at a reference temperature T_R. Because of the high dilution of the solutions studied, densities of the pure solvents were used in the calculations.

(58) Vargaftik, N. B.; Vinogradov, Y. K.; Yargin, V. S. *Handbook of Physical Properties of Liquids and Gases: Pure Substances and Mixtures*, 3rd ed.; Begell house Inc.: New York, 1996.

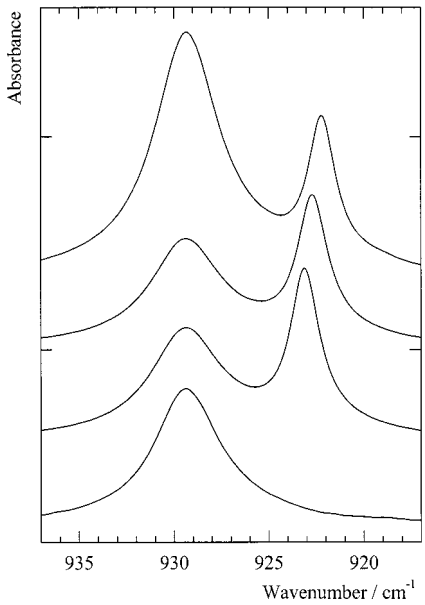

Figure 3. Infrared spectra of solutions in liquid krypton at 123 K, in the region of ν_6^{DME}, from top to bottom: solution containing dimethyl ether and $HCCl_3$, with mole fraction equal to 2.9×10^{-4} and 1.0×10^{-4}, respectively; solution containing dimethyl ether and $HCCl_2F$, with mole fraction equal to 1.0×10^{-4} and 0.9×10^{-4}, respectively; solution containing dimethyl ether and $HCClF_2$, with mole fraction equal to 1.2×10^{-4} and 1.1×10^{-4}, respectively; solution containing only dimethyl ether, with mole fraction equal to 1.3×10^{-4}.

For the present study, solutions, containing mole fractions typically 2×10^{-4} of DME and of the haloform, were recorded at several temperatures between 89 and 123 K in LAr and between 123 and 153 K in LKr. Band areas of the haloform CH stretches were determined by numerical integration. For $HCClF_2$, the band area of the complete doublet was used. For a Fermi resonance, the sum of the perturbed band areas equals the sum of the unperturbed band areas. The unperturbed band area of the overtone or combination band in resonance with the fundamental is usually at least an order of magnitude smaller than that of the fundamental, so that the error made by using the band area of the complete doublet is small.

For each temperature run, the plot of the corrected band areas of the monomer versus those of the complex invariably showed a high degree of linearity. Neglecting minor temperature variations of the infrared intensities, the ratio $\epsilon_{complex}/\epsilon_{monomer}$ was obtained as the slope of the linear regression line through the points of each plot. The values obtained have been collected in Table 1. It can be seen that within the uncertainty the results for $HCClF_2$ in LAr and LKr are identical. In contrast, a significant difference is found for $HCCl_2F$, which presumably reflects a weak solvent effect on the ratio. For $HCCl_3$, solubility problems prevented the ratio from being measured in LAr, so only the result for LKr is given.

The ratios show that the intensity of $\nu_1^{haloform}$ decreases slightly upon complexation for $HCClF_2$, by an average factor of 0.86(4), but that it increases for $HCCl_2F$ and $HCCl_3$, by an average factor of 33(3) in the former, and by a factor 56(3) in the latter. Hence, including the decrease by a factor 11(2) as determined[36] for HCF_3, there is a systematic trend, from decrease to increase in intensity, between HCF_3 and $HCCl_3$.

Ab Initio Calculations. Information on the equilibrium geometries and the relative stabilities of the complexes was

Table 2. Ab Initio Geometrical Parameters (Bond Lengths in Å, Bond Angles in deg) for Different Haloforms

	HCF_3		$HCClF_2$		$HCCl_2F$		$HCCl_3$	
geometrical data	monomer	complex	monomer	complex	monomer	complex	monomer	complex
C−H	1.0887	1.0874	1.0883	1.0875	1.0874	1.0876	1.0860	1.0875
C−Cl			1.7610	1.7680	1.7608	1.7647	1.7661	1.7688
C−Cl					1.7615	1.7666	1.7660	1.7687
C−Cl							1.7664	1.7697
C−F	1.3442	1.3482	1.3499	1.3530	1.3602	1.3629		
C−F	1.3442	1.3482	1.3499	1.3531				
C−F	1.3443	1.3486						
C−O	1.4156	1.4190	1.4156	1.4190	1.4156	1.4193	1.4156	1.4198
		1.4189		1.4199		1.4201		1.4201
van der Waals distance		2.2486		2.2096		2.1603		2.1105
O−Ĥ−C		176.1		167.6		170.1		176.2
C_{DME}−Ô−H		122.9		122.2		122.8		123.3
		125.8		126.6		125.9		124.8

Table 3. BSSE-Corrected Complexation Energies, in kJ mol^{-1}, Obtained for the Complexes Formed between Dimethyl Ether and HCF_3, $HCClF_2$, $HCCl_2F$, and $HCCl_3$

	MP2[a]	MP2[b]	MP2[c]
HCF_3	13.8	15.4	16.4
$HCClF_2$	15.6	17.2	17.2
$HCCl_2F$	16.9	18.4	18.1
$HCCl_3$	18.5	19.9	19.5

[a] MP2=FC/6-31G(d). [b] MP2=FULL/6-311++G(2d,2p)//MP2=FC/6-31G(d). [c] MP2=FULL/6-311++G(3df,2pd)//MP2=FC/6-31G(d).

obtained from BSSE-corrected gradient optimizations, at the MP2=FC/6-31G(d) level. The essential geometrical data and complexation energies are given in Tables 2 and 3, respectively.

For all complexes, the hydrogen bond between the haloform hydrogen and the oxygen atom is formed in the C−O−C plane of the ether. Table 2 shows that the van der Waals distance, that is, the O···H intermolecular distance, steadily decreases, from approximately 2.249 Å for the complex with HCF_3 to approximately 2.110 Å for DME·$HCCl_3$. The shortest distances between DME hydrogen atoms and haloform halogens are 3.77 (H···F), 3.55 (H···Cl), 3.57 (H···Cl), and 3.79 Å (H···Cl) for the complexes with HCF_3, $HCClF_2$, $HCCl_2F$, and $HCCl_3$, respectively. These distances are well above the sum of the van der Waals radii of the atoms involved,[59] and hence there are no indications for specific interactions other than that between the haloform hydrogen and the DME oxygen.

Because the hydrogen bonds are formed between the same two atoms, and because all data were obtained from the BSSE-corrected PES, the values for the O···H distance directly reflect the strength of the interaction. Thus, it is concluded that the strength of the interaction increases with the number of chlorine atoms present in the proton donor molecule. This trend is also seen in the calculated complexation energies which have been collected in Table 3. They can be seen to increase from 13.8 for DME·HCF_3 to 18.5 kJ mol^{-1} for DME·$HCCl_3$. It may be remarked that this is in line with what was concluded above from the behavior of ν_6^{DME} upon complexation.

The above complexation energies were obtained using a moderate basis set, so it cannot be excluded that they are influenced by basis set incompleteness errors (BSIE). An estimate for this was obtained by performing single point calculations at the MP2=FULL/6-311++G(2d,2p) and the MP2=FULL/6-311++G(3df,2pd) levels, using the geometries derived from the MP2/6-31G(d) BSSE-corrected PES. The resulting BSSE-corrected complexation energies are also given in Table 3. It shows that the energies increase with the size of the basis set, confirming that at the 6-31G(d) level the stabilities of the complexes are slightly underestimated as a consequence of BSIE. It is clear, however, that at all levels the same trend is found, with the $HCCl_3$ complex being the more stable.

The calculations predict that the formation of the complex decreases the haloform C−H bond length in HCF_3, by 13 × 10^{-4} Å, and in $HCClF_2$, by 8 × 10^{-4} Å, but increases the bond length in $HCCl_2F$, by 2 × 10^{-4} Å, and in $HCCl_3$, by 15 × 10^{-4} Å. For the former two and for $HCCl_3$ the change in C−H bond length, that is, the strengthening or weakening of the C−H bond, is in line with the observed shift of the C−H stretching, $\nu_1^{haloform}$. For $HCCl_2F$, however, a small increase of the bond length is calculated, while a small blue shift is observed.

The data in Table 2 also show that for all complexes the carbon−halogen bond lengths are slightly higher in the complex. These structural data are in line with the experimentally observed lowering of the carbon−halogen bond stretches.

For the complexes with HCF_3 and $HCCl_3$, the C−H···O bond angle is calculated close to 176°, while for the complexes with $HCClF_2$ and $HCCl_2F$ this angle is predicted to be significantly smaller. This behavior can be rationalized as the alignment of the haloform dipole moment with the electric field generated by the DME moiety; analysis shows that in all complexes the haloform dipole moment is very nearly collinear with the electric field vector generated by DME at the haloform center of mass, the deviations being less than 0.5°.

The vibrational frequencies and infrared intensities of monomers and complexes, calculated in the harmonic approximation, and their assignments, are collected in Tables S3 and S4 of the Supporting Information. Comparison with the experimental data in Tables S1 and S2 shows that, despite the moderate basis set, the agreement between theory and experiment is surprisingly good.

Discussion

The spectroscopic results on the DME complex with HCF_3[36] complement the present ones, so that an interesting series is obtained. Therefore, in the following paragraphs we will systematically include that complex in our discussion.

The Hydrogen Bond Index. Hydrogen bonding has been described[14] as a process in which electron density is transferred from the electron donor to the X−H antibonding σ^* orbital. In

(59) Gillespie, R. J.; Popelier, P. L. A. *Chemical Bonding and Molecular Geometry*; Oxford University Press: Oxford, 2001; p 115.

Table 4. Electron Density Transfer (in e) and H-Index for the Complexes between Dimethyl Ether and Different Haloforms

	HCF_3	$HCClF_2$	$HCCl_2F$	$HCCl_3$
EDT	0.0108	0.0119	0.0144	0.0176
$\Delta\sigma^*$	0.0016	0.0023	0.0037	0.0058
H-index	0.1518	0.1933	0.2568	0.3294

the NBO analysis of ab initio calculations on improper hydrogen bonding, it has been observed that there is substantial additional charge transfer.[15,35,36] This has triggered the definition of a so-called H-index that should allow one to unambiguously discriminate between classical, red-shifting and improper, blue-shifting hydrogen bonding.[14] The H-index is defined as the ratio of electron density (ED) transferred to X−H and the total ED transfer between electron and proton donor. On the basis of a number of calculations, it was suggested that the value of the index for proper hydrogen bonding lies between 1.0 and 0.7, while for improper hydrogen bonding it should fall between 0.0 and 0.3.[14] For the present complexes, the values of the H-index have been calculated from a full natural bond orbital analysis using the MP2 density matrix.[60] The results are given in Table 4. For the blue-shifting complexes, those of HCF_3 through $HCCl_2F$, the H-index can be seen to be within the boundaries set by Hobza,[14] but for the chloroform complex, with its clear red shift and intensity increase, the H-index, 0.329, is very close to the range proposed for improper, blue-shifting hydrogen bonding. The result for the latter complex suggests that the strict limits in H-index values proposed for both types of hydrogen bonding[14] must be relaxed.

The Electric Field Effect. In a hydrogen-bonded dimer, the proton donor is exposed to the electric field of the acceptor. The systematics of the influence of a homogeneous electric field on the vibrational frequency and infrared intensity of the O−H stretching of water have been investigated by K. Hermansson.[61] In that study, it was shown that, depending on the field, the vibrational frequency can show a downward or an upward shift. More recently, along the same lines, the influence of a homogeneous electric field, simulating the field of the proton acceptor[12] on the C−H stretching of the donors HCN, acetylene, and methane, has been calculated. The field was taken parallel to the dipole of H_2O as the electron donor. At a field strength appropriate for H_2O, the C−H bond length in acetylene and HCN is longer than that in the corresponding field-free molecules, while in methane it is shorter; these changes are in agreement with the ab initio predictions on the complexes in which these proton donors are hydrogen bonded to the oxygen atom of H_2O. Although a homogeneous field is only the zeroth approximation to the real electric field generated by the proton acceptor, this result suggests that the dominant fraction of the C−H bond length behavior is due to straightforward electrostatic polarization of the proton donor. Because changes in the C−H bond length directly reflect the complexation shift of the stretching frequency, we have investigated if the present hydrogen bonds can be discussed in terms of this model. For the calculations, the approach of Masunov et al.[12] was used; that is, the structure of the proton donor was optimized at the MP2=FC/6-31G(d) level, using Gamess,[62] in a uniform electric field oriented parallel to the dipole of DME. The C−H bond

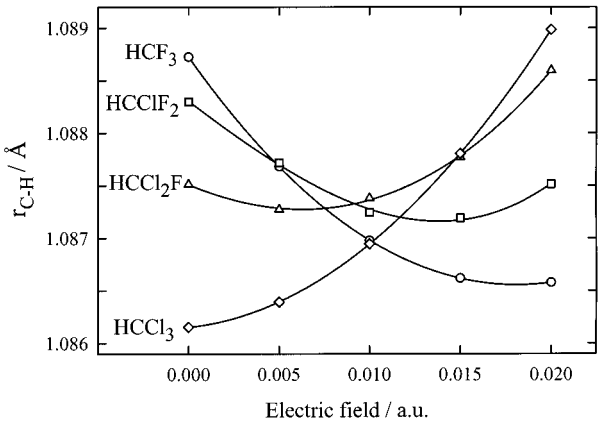

Figure 4. C−H bond lengths of haloforms subjected to a uniform electric field, as a function of positive field strength.

lengths as a function of positive field strength are collected in Figure 4; the calculated points for each proton donor have been connected with a third order polynomial, which is shown as a solid line. The strength of the actual electric field generated by DME is not uniform, but decreases rapidly with increasing distance from DME; at a point corresponding to the position of the haloform proton in the present complexes, the field strength is close to 0.02 au, while at a point corresponding to the midpoint of the haloform C−H bond in the complexes, the field strength has decreased to approximately 0.01 au. The strength of the uniform field used in the calculations of Masunov et al.[12] was taken to be the value at the former point. Making this choice for the present complexes, Figure 4 shows that the C−H bond length decreases for HCF_3 and $HCClF_2$, while for $HCCl_2F$ and $HCCl_3$ it increases. For the former two, and for chloroform, these changes are consistent with the observed complexation shifts, that is, a bond length decrease leading to a blue shift and vice versa. For $HCCl_2F$, however, the increase of the C−H bond length predicted from Figure 4 is in contradiction with the experimental blue shift.

Because of the inhomogeneous nature of the field generated by DME, there is no reason the choice of field strength by Masunov et al.[12] should give the superior results. Therefore, one may equally well choose the field strength of the second point, at the midpoint of the haloform C−H bond. It can be seen in Figure 4 that at this strength of the uniform field the direction of the C−H stretch shifts is correctly predicted for all haloforms. Despite the ambiguity in the choice of the field strength, it is clear from these calculations that the direction of the complexation shift of the C−H stretching frequency is dominated by the electric field effect induced by the electron donor.

It would evidently be better to simulate the electric field of DME by an inhomogeneous one. The latter could be generated, for instance, through a background charge distribution consisting of a series of point charges positioned at the atomic centers of DME. The study of the influence of an inhomogeneous field on the structure of a molecule is, however, not straightforward; without constraining the molecule, structure optimization causes it to collapse onto the background distribution. Several pos-

(60) Reed, A. E.; Curtiss, L. A.; Weinhold, F. *Chem. Rev.* **1988**, *88*, 899.
(61) Hermansson, K. *J. Chem. Phys.* **1993**, *99*, 861.
(62) Schmidt, M. W.; Baldridge, K. K.; Boatz, J. A.; Elbert, S. T.; Gordon, M. S.; Jensen, J. H.; Koseki, S.; Matsunaga, N.; Nguyen, K. A.; Su, S. J.; Windus, T. L. *J. Comput. Chem.* **1993**, *14*, 1347.

sibilities for constraints have, therefore, been investigated.[63,64] Obvious ones for the present purpose would be to keep constant either the van der Waals bond length or the distance between the haloform carbon and the oxygen atom. With the former constraint, the carbon atom relaxes toward the oxygen atom; with the latter one, the hydrogen atom is shifted in the same direction. Thus, the behavior of the C−H bond is determined by the constraint, which prevents the correct insight to be derived from the structure optimizations. As the actual constraint in the complex is the exchange repulsion barrier between the monomers, the alternative would be to simulate that barrier by, among other possibilities, the $1/r^{12}$ term of the Lennard-Jones potential. This potential barrier will influence the structure into which the haloform relaxes, so that, apart from the problems with modeling the evolution of the barrier in the series of haloforms, isolation of the field influence is no longer possible. Therefore, in the present study no attempts were made to optimize the haloform structure in an inhomogeneous field.

An inhomogeneous field without structure optimization, however, was used to more realistically describe the field influence on the haloform electron distribution and on the infrared intensity of haloform C−H stretching, described in the following paragraphs. The electric charges for this distribution were calculated for monomer DME, using the CHELP subroutines in Gaussian,[40] in which the charges are optimized to reproduce the electric field and the dipole moment of the molecule. For the calculations, the distances between the haloform hydrogen atom and the charge replacing the DME oxygen atom were taken to be the ab initio H···O van der Waals distances as given in Table 2. The choice of charges used here ensures that the electric field is a good approximation to that of the isolated DME. To simulate the electric field of DME as it is generated by this monomer in the complex would be better still; such calculations are not possible with the available subroutines, and for the present qualitative purposes this improvement, therefore, was not further pursued.

The above analysis has shown that the electric field effect on the proton donor is responsible for the contraction of the C−H bond, and thus for improper, blue-shifting hydrogen bonding. This is in contrast with the hypothesis[15,35,36] that improper hydrogen bonding is the *consequence* of charge transfer to the remote part of the molecule. Such a charge transfer, to, for instance, lone-pair orbitals on the fluorine atoms in fluoroform complexes, has been inferred from NBO analysis before.[13] Chemical intuition suggests that their remoteness makes it unlikely that there is direct transfer of electrons from the electron donor to such orbitals. As a matter of fact, the increased population of these orbitals is not caused by actual charge transfer, but is a mere consequence of the electric field effect on the proton donor. This is illustrated by the electron density difference maps in Figure 5, that were calculated at the MP2=FC/6-31G(d) level. The map shown on the left-hand side was obtained by point-to-point subtraction of the ab initio electron density of monomer HCF_3 from that of HCF_3 in the DME complex. The map on the right-hand side was similarly obtained from the densities of monomer HCF_3 and the densities of HCF_3 exposed to the background charge distribution. All calculations were made using the geometry of HCF_3 as optimized in the full complex.

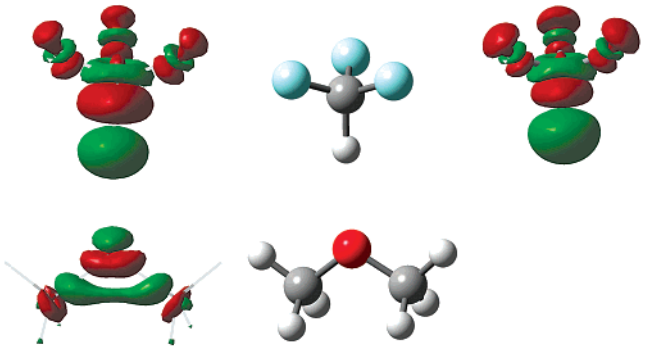

Figure 5. Electron density difference maps of DME·HCF_3: (left) point-to-point subtraction of the ab initio electron density of monomer HCF_3 from that of HCF_3 in the complex; (right) subtraction of the ab initio electron density of monomer HCF_3 from that of HCF_3 exposed to a background charge distribution. The regions of increased electron density are shown in red; those with decreased electron density are shown in green. The density used for plotting the surfaces is ± 0.0004 e/a_0^3.

The patterns of density loss and gain in fluoroform are very similar in both maps, and are also similar to those obtained by Scheiner et al.[37] for a series of C−H···O complexes with water as the proton acceptor. The latter similarity suggests that the choice made above for the inhomogeneous field is not of crucial importance. The density gain in the fluorine lone pairs present in rather the same way in both maps of Figure 5 proves our point, that this gain is due to the electric field effect on the proton donor.

Finally, it may be remarked that the vibrational spectra give indirect evidence for the involvement in the complexation of orbitals located on the halogens; it was shown above that for all haloforms the carbon−halogen stretches are significantly shifted by the complexation. As the carbon−halogen bonds do not participate in the formation of the complex bond, these shifts testify of changes in the electronic characteristics of the carbon−halogen bonds.

Infrared Intensities. The other aspect usually associated with improper hydrogen bonding by a C−H bond[3,8,10,15] is the decreased infrared intensity of the C−H stretching vibration. It is clear from Table 1 that for the present series of proton donors a systematic trend in the relative intensity of this vibration is found, with the blue-shifting HCF_3 and $HCClF_2$ giving a decrease in the intensity of ν_1, and the red-shifting $HCCl_3$ giving an increase. The exception is $HCCl_2F$, which gives a blue shift for ν_1, but sees its intensity increase by a factor 30. This illustrates that there is not a one-to-one correspondence between the two aspects.

Some insight into the intensity phenomenon was gained from ab initio calculations on the fluoroform and chloroform complexes, in the following way. Consider the monomers as they occur in their complex. The haloform CH stretching superposes an oscillatory component, characterized by a gradient $(\partial\vec{\mu}/\partial Q_1)_o$, on the dipole moment of the haloform. Because of the DME electric field effect on the haloform, this gradient not necessarily bears a direct relation to the gradient for ν_1 of the free haloform. The haloform oscillatory component induces an equally oscillatory component on the dipole moment of DME. The symmetry and structure of the complexes are such that the gradient induced in DME is parallel to the inducing gradient in the haloform.

(63) Kairys, V.; Head, J. D. *J. Phys. Chem. A* **1998**, *102*, 1365.
(64) Kairys, V.; Head, J. D. *Chem. Phys. Lett.* **1998**, *288*, 423.

Consequently, their vector sum is longer than the inducing gradient itself. Hence, the role of DME is to *increase* the intensity of ν_1 in the complex.

The above shows that a decreased intensity, as in the case of fluoroform, must be due to the fact that in the complex the inducing gradient is much smaller than the corresponding gradient of free fluoroform. Within the framework of the above model, this must be due to the electric field effect on the haloform. This can be verified from a comparison of the ν_1 gradient in free haloform with that for the haloform exposed to the field of the background charge distribution. These gradients were calculated approximating the ν_1 normal coordinate by the C−H stretch internal coordinate. For the free haloform, the gradient was calculated around the relaxed monomer ab initio structure, while for the haloform exposed to the inhomogeneous field, it was calculated around the ab initio structure as it was optimized for the full complex. In each case, the dipole moment was calculated for this central structure and for four others, in which the hydrogen was displaced along the C−H bond direction by 0.05 and 0.1 Å in either direction. As before, the calculations were performed at the MP2=FC/6-31G(d) level. The direction cosine of the polynomial regression through the dipole moments at the zero displacement H-position was identified with the gradient for ν_1. The values resulting from these calculations are −0.434 D Å^{-1} for free HCF_3, and −0.042 D Å^{-1} for field-exposed HCF_3. The negative value for the free haloform, that is, the decrease of the dipole moment with increasing C−H bond length, is in line with previous calculations.[65] The predicted infrared intensity ratio I_{field}/I_{free} is obtained by squaring the ratio of these gradients, and equals 0.009. A similar calculation for the chloroform complex leads to gradients of 0.131 and 0.621 D Å^{-1} for free and field-exposed $HCCl_3$, respectively, leading to a value of 22.5 for the intensity ratio. Comparison with the data in Table 1 shows that the ratio for fluoroform, 0.009, is in reasonable agreement with the ab initio value of 0.024. For chloroform the agreement is less good, as the ab initio ratio equals 3877. The high value of the latter undoubtedly is a consequence of the very small ab initio infrared intensity for free $HCCl_3$; relative to the ab initio values for the other modes this small intensity is in contradiction with the observed relative intensities, and hence must be an artifact of the ab initio calculation. Compared with the experimental intensity ratios, also given in Table 1, the result for chloroform is in reasonable agreement, the experimental ratio being 56(3). For fluoroform, the agreement is less good, as the model predicts a decrease of the ν_1 intensity of the complex which is nearly an order of magnitude greater than experimentally observed. All in all, however, it is clear that for both haloforms the experimental trend is reproduced by the model, while its simplicity, combined with the sensitivity of the dipole gradient to small structural changes, most likely accounts for the discrepancies with the experimental values. We, therefore, conclude that the electric field effect of the proton acceptor on the proton donor may be held largely responsible for the observed changes of the C−H stretch intensity. This conclusion is in line with that from an ab initio analysis of the $H_3N{\cdot}HCl$ complex,[66] in which the intensity behavior of ν_{HCl} was rationalized in terms of the "equilibrium charge−charge flux model". It was shown that in the complex the intensification is due to an important charge flux, which is almost absent in monomer HCl. This flux was interpreted to be due to the repulsion between the electrons in the H−Cl bond by the NH_3 lone pair, which amounts to saying that in the complex the proton donor HCl is influenced by the electric field generated by the proton acceptor.

(65) Hobza, P.; Havlas, Z. *Chem. Phys. Lett.* **1999**, *303*, 447.

Conclusions

In this study, we have presented the results of an infrared study of mixtures of haloforms of the type $HCCl_nF_{3-n}$ (n = 1−3) with dimethyl ether, dissolved in liquid argon and/or liquid krypton. Each haloform was observed to form a 1:1 complex with the ether.

For $HCClF_2$ and $HCCl_2F$, the complexation was observed to induce a blue shift for the haloform C−H stretching fundamental, while for $HCCl_3$, a red shift was observed. For $HCClF_2$, the complexation is accompanied by a decrease of the band area of the same mode, while for $HCCl_2F$ and $HCCl_3$, the band area is increased. The trends in frequency and intensity are reproduced by the ab initio calculations on the complexes in which the structures are optimized on the BSSE-corrected potential energy surface.

For the analysis of the results, the recent observations on the complex of HCF_3 with dimethyl ether have also been considered. By performing calculations on the haloforms embedded in homogeneous electric fields, it is shown that, in the series of haloforms studied, the evolution from blue to red shift of the haloform C−H stretching frequency, and from decrease to increase of the infrared intensity of the same mode, is largely due to the electric field effect induced by the electron donor.

Acknowledgment. S.N.D. thanks the FWO-Vlaanderen for an appointment as a research assistant. Gratitude is expressed to the FWO-Vlaanderen for their assistance toward the purchase of spectroscopic equipment used in this study. The authors thank the Flemish Community for financial support through the Special Research Fund (BOF).

Supporting Information Available: Tables S1 and S2 report the observed infrared frequencies and complexation shifts, in cm^{-1}, for the different haloforms and dimethyl ether, respectively. Tables S3 and S4 give the MP2=FC/6-31G(d) infrared frequencies, infrared intensities, and complexation shifts for the haloforms and dimethyl ether modes, respectively (PDF). This material is available free of charge via the Internet at http://pubs.acs.org.

JA0125220

(66) Szczesniak, M. M.; Kurnig, I. J.; Scheiner, S. *J. Chem. Phys.* **1988**, *89*, 3131.